Exploring the structure-activity relationship of benzylidene-2,3-dihydro-1H-inden-1-one compared to benzofuran-3(2H)-one derivatives as inhibitors of tau amyloid fibers

Emeline Boukherrouba, Camille Larosa, Kim-Anh Nguyen, Jérémy Caburet, Laurent Lunven, Hugues Bonnet, Antoine Fortuné, Ahcène Boumendjel, Benjamin Boucherle, Sabine Chierici, et al.

Exploring the structure-activity relationship of benzylidene-2,3-dihydro-1*H*-inden-1-one compared to benzofuran-3(2*H*)-one derivatives as inhibitors of amyloid fibers

Emeline Boukherrouba[a,†], Camille Larosa[b,†], Kim-Anh Nguyen[a], Jérémy Caburet[a], Laurent Lunven[a,b], Hugues Bonnet[b], Antoine Fortuné[a,1], Ahcène Boumendjel[a,2], Benjamin Boucherle[a], Sabine Chierici[b,‡], Marine Peuchmaur[a,‡,*]

[a]Univ. Grenoble Alpes, CNRS, DPM, 38000 Grenoble, France
[b]Univ. Grenoble Alpes, CNRS, DCM, 38000 Grenoble, France

*Corresponding author Tel.: +33476635295; fax: +33476635298.
E-mail address: marine.peuchmaur@univ-grenoble-alpes.fr

ABSTRACT

Tauopathies, such as Alzheimer's disease, have been the subject of several hypotheses regarding the way to treat them. Hyperphosphorylation of tau protein leading to its aggregation is widely recognized as a key step in the development of these diseases resulting in neuronal dysfunction. The AcPHF6 model of tau that includes the shorter critical fragment involved in the protein aggregation was used *in vitro* to identify new potential inhibitors. Following a previous study on aurone derivatives, we herein compare this polyphenol family to a very close one, the benzylidene-2,3-dihydro-1*H*-inden-1-one (also named indanone). The structure activity relationship studies bring to light the importance of the hydroxylation pattern in both series: the more hydroxylated, the more active. In addition, the three-dimensional shape of the molecules is involved in the way they interact with their target, thus defining either a role as an inhibitor of fiber elongation or as a chemical probe of fibers. Compound **13a** was identified as a promising inhibitor: its activity was confirmed by circular dichroism and atomic force microscopy studies.

Keywords: Indanones; Aurones; Alzheimer's disease; tau aggregation; AcPHF6 peptide.

† Both junior investigators equally contributed to the work.
‡ Both senior investigators equally contributed to the work.
[1] Current affiliation: Univ. Cote d'Azur, CNRS, iBV, 06000 Nice, France
[2] Current affiliation: Laboratoire des Radiopharmaceutiques Biocliniques, Faculté de Médecine, Université Grenoble Alpes

1. Introduction

Tau, the major hydrophilic microtubule-associated protein (MAP), is involved in the normal brain function, playing a crucial role in the assembly and stability of microtubules. In Alzheimer disease (AD) and in the other related neurodegenerative diseases, known as tauopathies, tau is abnormally hyperphosphorylated. The subsequent conformational changes of this protein ultimately lead to the formation of highly disruptive and toxic intracellular aggregates, and then neurofibrillary tangles (NFTs) [1–3]. Their deposition in the brain results in neuronal dysfunction and eventually death of neurons, but the pathophysiological role of tau protein, notably in AD, is still not fully understood. Nevertheless, the shorter critical fragment prominently involved in tau aggregation was previously identified and was referred to as PHF6 [4]. To go further in the understanding of tau aggregation mechanism, an hexapeptide model was also developed: the AcPHF6 derivative (Ac-VQIVYK-NH_2). It is able to undergo efficient *in vitro* fibrillation to form cross β-sheet structures and paired helical filaments very similar to those of pathological full-length tau [5,6]. The inhibition of the aggregation process of tau representing a relevant therapeutic target for tauopathies, this model was mainly used for the prompt biochemical evaluation of new inhibitors [7–10] but it can also be useful for the search of probes that could participate in AD treatment or diagnosis [11].

A few years ago, we explored the interaction between diverse polyhydroxylated benzylidene aurones (Fig. 1) and the tau model AcPHF6 [11]. Firstly, this study showed that at least four groups are needed to achieve significant activity. Depending on the hydroxylation pattern, it also revealed that aurones may act as inhibitors of fiber elongation or as chemical probes of fibers. While pursuing our investigation, we focused our efforts on hydroxylated benzylidene indanones which are structurally very close to aurones.

Indanones are very useful precursors involved in the synthesis of diverse natural or synthetic heterocyclic molecules, including the probably most significant drug bearing an indanone moiety, donepezil, an acetylcholinesterase inhibitor approved for the treatment of AD (Fig. 1) [12,13]. Arylidene indanones are both closely related to aurones and chalcones (Fig. 1), incorporating the α,β-unsaturated ketone moiety of the latter in a rigid five-membered ring. Indanones are also one of the privileged structures in medicinal chemistry associated with a broad spectrum of biological activities such as anti-inflammatory, antimicrobial, antiviral or anticancer activities [14–16]. More specifically, 2-arylidene indanone derivatives have been investigated on various biological targets related to AD, such as acetylcholinesterase inhibitors, metal-chelating agents, potential probes for β-amyloid plaques even, logically, as multi-target-directed ligands against AD [17–20]. To the best of our knowledge, there is currently no evidence of interaction between tau and this family of compounds.

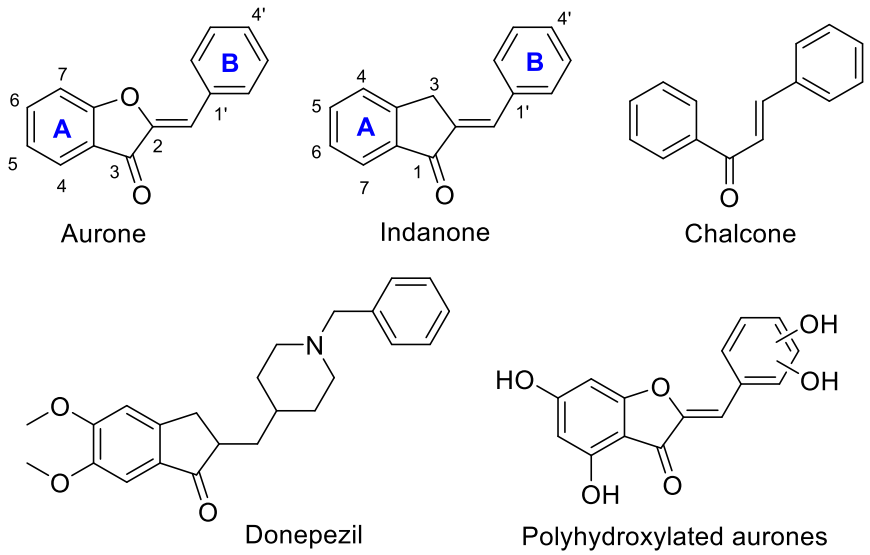

Fig. 1. General structure of aurone, chalcone and indanone backbones (top); structures of donepezil and representative polyhydroxylated aurones previously studied [11] (bottom).

Herein, this paper reports the design, synthesis and amyloid fibers interaction of benzylidene-2,3-dihydro-1*H*-inden-1-one derivatives and their benzofuran-3(2*H*)-one analogues. The tau AcPHF6 model, using thioflavin T (ThT) fluorescence assays, circular dichroism (CD), and atomic force microscopy (AFM) were used to assess and compare the effect of the two families of compounds on amyloid fibers.

2. Chemistry

Indanones were prepared according to known procedures starting with the synthesis of the suitably substituted 2,3-dihydro-1*H*-inden-1-one derivatives **2** and **6** (scheme 1). The hydroxylation pattern of indanones were mostly chosen to obtain corresponding analogues of previously synthesized aurones [11]. 4-Hydroxy-2,3-dihydro-1*H*-inden-1-one **2** was thus obtained thanks to a Friedel-Crafts acylation starting from commercially available chroman-2-one **1** in the presence of $AlCl_3$ [21]. Compound **6**, 5,7-dimethoxy-2,3-dihydro-1*H*-inden-1-one, was prepared from 3,5-dimethoxybenzaldehyde **3** and malonic acid *via* the Doebner modification of the Knoevenagel condensation [22]. The α,β-unsaturated carboxylic acid **4** was subsequently hydrogenated to give compound **5** which was finally cyclized in the presence of methanesulfonic acid (MSA) [23].

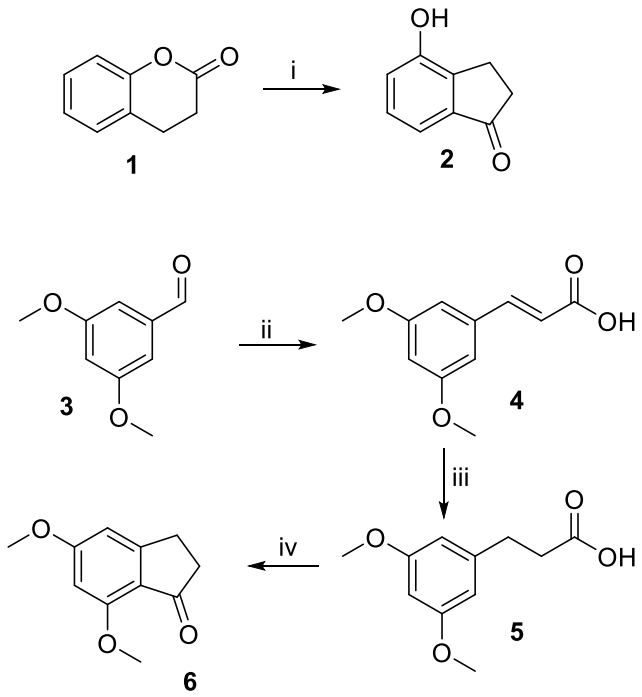

Scheme 1. Synthesis of the indanone cores **2** and **6**. Reagents and conditions: (i) $AlCl_3$, NaCl, 200 °C, 1 h, 55%; (ii) malonic acid, pyridine, piperidine, 100 °C, 6 h, 94%; (iii) H_2, HCO_2NH_4, 10% Pd/C, EtOH, rt, 16 h, 40%; (iv) MSA, 95 °C, 6 h, 44%.

The 2,3-dihydro-1*H*-inden-1-one derivatives **2** and **6** described above and the commercially available 2,3-dihydro-1*H*-inden-1-one **7** were then condensed with benzylaldehyde derivatives in basic conditions to give the corresponding indanones (**11a-o**, scheme 2 and table 1). When the condensation was carried out with methoxylated 2,3-dihydro-1*H*-inden-1-one and/or benzaldehyde derivatives, the hydroxyl analogues were obtained by reaction of intermediates **11** with BBr_3 in dry dichloromethane to give **13a-b** and **13g-o**.

To complete our set of indanone and aurone analogue derivatives, diverse polyhydroxylated aurones were synthesized (**12a-c**, **e-g**, **i-o** and **14a-b**, **i**, **m-o**, table 1) following the same procedure as described for indanones (scheme 2). The synthesis of benzofuran-3(2*H*)-ones **8**, **9a**, **9b** and **10** used as starting materials were already described [11].

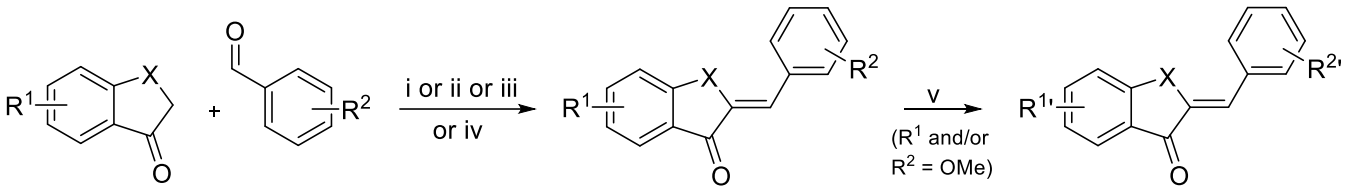

2 (X = CH_2, R^1 = 4-OH)
6 (X = CH_2, R^1 = 5,7-OMe)
7 (X = CH_2, R^1 = H)
8 (X = O, R^1 = 7-OMe)
9a (X = O, R^1 = 4,6-OH)
9b (X = O, R^1 = 4,6-OMe)
10 (X = O, R^1 = H)

11a-o (X = CH_2)
12a-c, e-g, i-o (X = O)

13a-b, g-o (X = CH_2)
14a-b, i, m-o (X = O)

Scheme 2. Synthesis of indanone and aurone derivatives. Reagents and conditions: (i) X = CH_2: NaOH aq. 5%, EtOH, rt, 24–94%; (ii) X = O: Al_2O_3, dry CH_2Cl_2, rt, 6–92%; (iii) X = O: KOH aq. 50%, MeOH, 70 °C (MW), 50–82%; (iv) HCl, EtOH, 75 °C, 17% (for **12g**); (v) BBr_3, dry CH_2Cl_2, 24–72 h, 0 °C to rt, 30–100%.

Table 1

Structures of evaluated indanone and aurone derivatives. All the synthesized intermediates are not listed in this table (cf. experimental section).

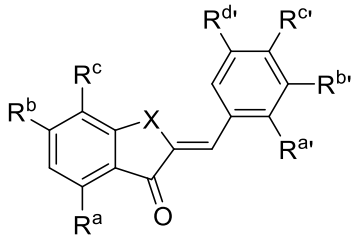

Indanone (X = CH_2)	Aurone (X = O)	R^a	R^b	R^c	$R^{a'}$	$R^{b'}$	$R^{c'}$	$R^{d'}$
11a	**-**	H	H	H	H	OMe	OMe	OMe
11b	**-**	H	H	OH	H	OMe	OMe	OMe
11c	**12c**	H	H	H	H	H	H	H
11d	**-**	H	H	H	H	OH	H	H
11e	**12e**	H	H	OH	H	H	H	H
11f	**12f**	H	H	OH	H	OH	H	H
13a	**14a**	H	H	H	H	OH	OH	OH
13b	**14b**	H	H	OH	H	OH	OH	OH
13g	**12g**	H	H	H	H	OH	H	OH
13h	**-**	H	H	OH	H	OH	H	OH
13i	**14i**	H	H	OH	OH	OH	OH	H
13j	**12j**	OH	OH	H	H	H	H	H
13k	**12k**	OH	OH	H	H	OH	H	H
13l	**12l**	OH	OH	H	H	OH	H	OH
13m	**14m**	OH	OH	H	OH	H	OH	H

13n	**14n**	OH	OH	H	H	OH	OH	H
13o	**14o**	OH	OH	H	H	OH	OH	OH

3. Results and discussion

3.1. Screening of aurones and indanones by thioflavin T fluorescence assays.

Thioflavin T (ThT) fluorescence assays were used to evaluate the potential inhibition activity of aurone and indanone derivatives toward the aggregation process of the tau AcPHF6 model [24,11]. Screening of compounds was carried out in 96-well microplates. The aggregation kinetics of the AcPHF6 peptide was recorded in phosphate buffer over 2 h in the presence of the ThT dye and of the synthesized compounds at 10 µM or 1 µM, corresponding to a peptide to compound ratio of 10:1 and 100:1, respectively. Results reported in figure 2 are expressed as the percentage of ThT fluorescence inhibition, the tau model AcPHF6 without potential inhibitors being used as control (see Fig. S1 for kinetics in presence of **11e** and **12e** as an illustration).

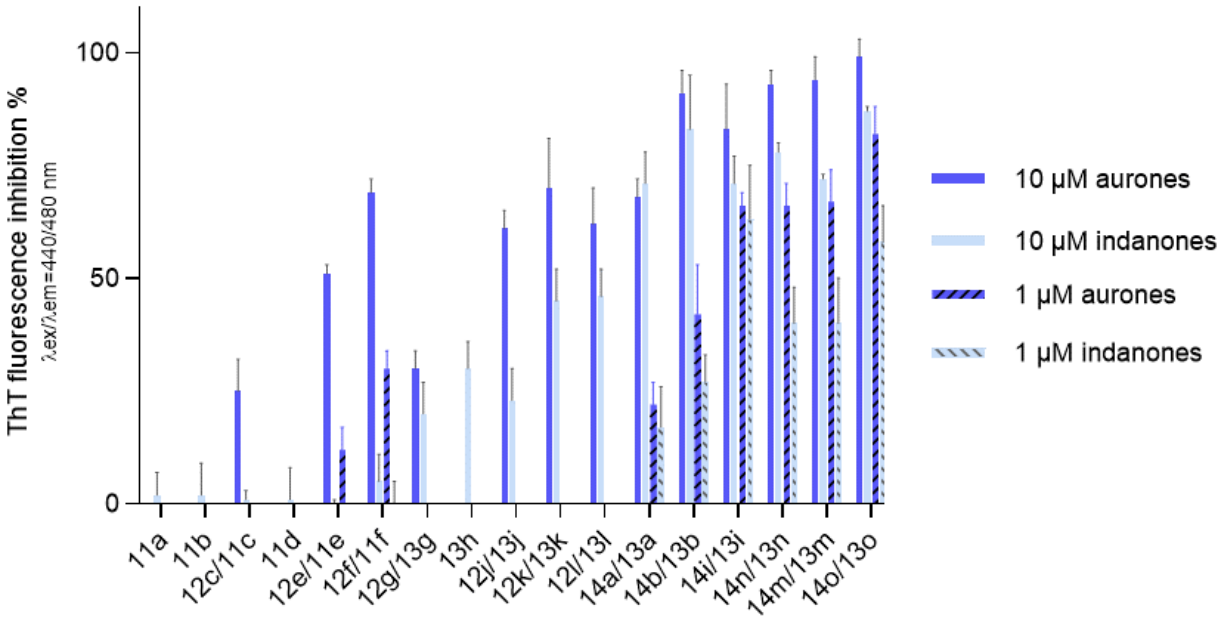

Fig. 2. ThT fluorescence inhibition (%) is obtained from ThT assay using 100 µM AcPHF6 and 10 µM ThT in 50 mM phosphate buffer pH 7.4. All assays were performed at least in triplicate and each bar value corresponds to the mean ± SD (λex and λem: wavelengths of excitation and emission).

To avoid misleading interpretations, it was first necessary to study the spectroscopic properties of tested compounds, i.e. absorbance and fluorescence. ThT assay is based on the fluorescence of the ThT dye in presence of the characteristic β-sheet motif of amyloid fibers in formation. Thus, it may be biased by an inner filter effect of molecules which strongly absorb in the same range as the bound ThT (wavelengths of excitation and emission at 440 and 480 nm, respectively) [25,26]. In

light of this, we recorded the UV/Vis absorption of all the molecules to check if their own spectroscopic properties would not interfere with the assays (Fig. 3). The UV/Vis spectra of indanones and their corresponding aurone derivatives are quite similar. Interestingly, the intensity and maximum absorption appeared to be lower for the indanone analogues. The highest absorption is observed for indanones **13m** and **13n** and their aurone analogues **14m** and **14n** with a maximum around 400-410 nm. It is noteworthy that these compounds along with the other ones from table 1 have a low absorption at 10 µM and 1 µM that cannot significantly quench the ThT fluorescence at the working wavelengths of the ThT assays. As for the intrinsic fluorescence of compounds, such emission was corrected by using blank wells and it remains very low at 480 nm when excited at 440 nm in comparison to the bound ThT fluorescence (Fig. S2). Furthermore, aurones and indanones do not exhibit any significant change in their emission spectra in the presence of preformed AcPHF6 fibers, except for indanones **11e** and **13b** (Fig. S3). Both indanones show no fluorescence on their own but a slight fluorescence emission when added to preformed fibers. The intensity is nevertheless low compared to the ThT fluorescence intensity and could only weakly undervalue the effect of both compounds. Remarkably, their corresponding aurones **12e** and **14b** do not show such behavior which may indicate a closer interaction with fibers of the indanone series.

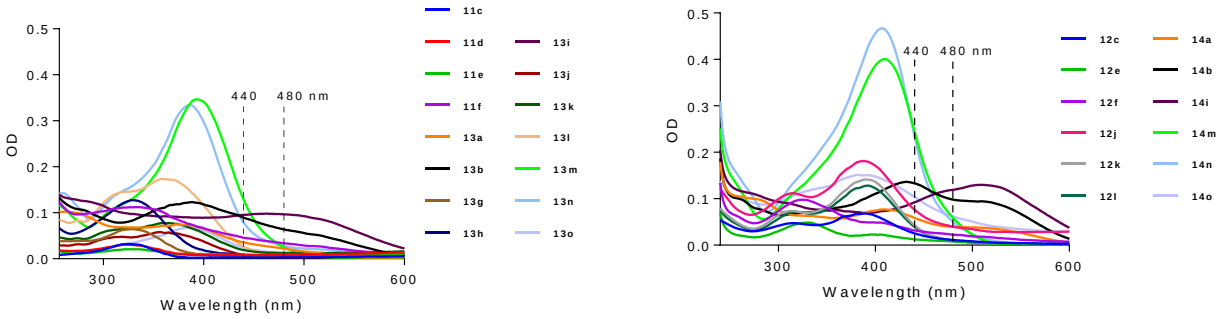

Fig. 3. (A) UV–Vis absorption spectra of indanones (left) and aurones (right). The spectra were recorded at 10 µM of compounds in 50 mM phosphate buffer in presence of 0.5% of DMSO.

Interestingly, aurone and indanone analogues displayed similar inhibitory activities at 10 µM with few exceptions (compounds **11e**/**12e**, **11f**/**12f** and **13j**/**12j**, Fig. 2). As expected, *O*-methylated indanones **11a**-**b** and unsubstituted indanones **11c** turned out to be inactive while unsubstituted aurone analogue **12c** showed a very weak activity at 10 µM. Contrariwise, modest to significant activities were obtained for more polar compounds. Nevertheless, monohydroxylated indanones **11d** and **11e** were inactive, unlike the corresponding aurone **12e** of the latter exhibited a higher, although still modest, activity. On the whole, increasing the number of hydroxyl groups on ring A and/or B appeared favourable to the inhibition properties of these classes of compounds, the most potent compounds being the tetra and pentahydroxylated ones (e.g. **13o**/**14o** and **13b**/**14b**). The hydroxyl group position on the B ring also influenced the potency of the inhibition, notably in the 4,6-dihydroxy series (comparison of compounds **13l**/**12l**,**13m**/**14m**, **13n**/**14n**, and **13o**/**12o**) in

which a substitution on the R4' position seems appropriate to maximize the desired interaction. These results are thus consistent with those obtain for polyhydroxylated aurones in our previous study [11].

A screening was carried out with a 1 µM concentration to further assess the most potent, and some 'atypical' pair of indanone/aurone compounds (Fig. 2). While the most potent compounds were still able to inhibit the ThT signal at 1 µM, the difference observed for the 'atypical' aurone/indanone pairs (**11e/12e** and **11f/12f**) was again clearly noticeable.

3.2. Displacement of bound ThT by fluorescence assay.

It is noteworthy that inhibition of fluorescence in ThT assays does not necessarily mean inhibition of amyloid aggregation process. Indeed, displacement of the bound ThT by the tested compounds may also occur. Thus, we recorded the emission spectrum of a solution of preformed AcPHF6 fibers in the presence of ThT right after adding an aurone or an indanone (Fig. 4).

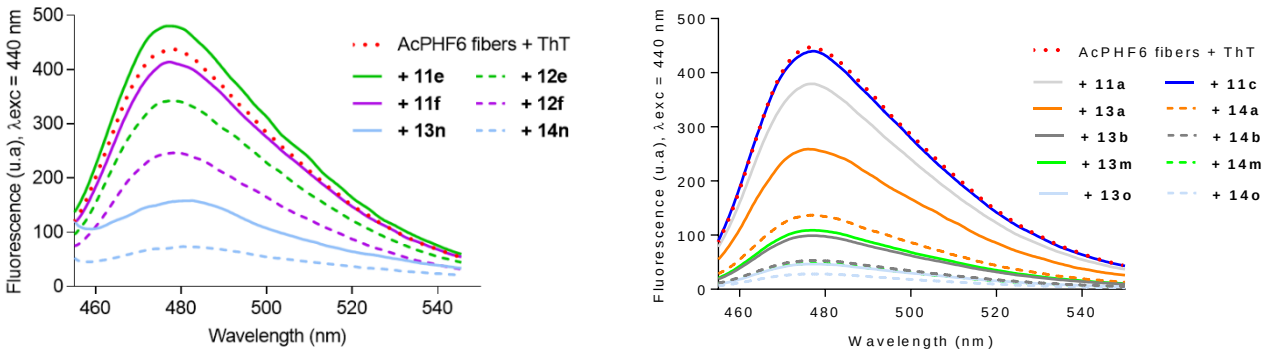

Fig. 4. ThT displacement assays. The ratio compound/ThT is 1:1 and the AcPHF6 fibers were prepared from 100 µM of peptide in presence of 10 µM ThT in 50 mM phosphate buffer pH 7.4. The excitation wavelength was 440 nm.

All active compounds in ThT assays induce a decrease in ThT fluorescence when added to preformed fibrils (e.g. **13a/14a**, **13b/14b**, **13m/14m**, **13n/14n**, **13o/14o**, **12f**). These results suggested that displacement of the bound ThT by the tested compounds in previous assay may also occur in place of or in competition with an inhibitory effect. Considering the short period of time left for this analysis, it is unlikely that the decrease of fluorescence signal was due to the disaggregation of fibers. To note, a slight increase of the fluorescence signal was observed after the addition of inactive compound **11e** to fibers. This could however be explained by the fluorescence emission of **11e** in presence of preformed fibers as mentioned earlier (Fig. S3).

3.3. Inhibition properties.

The inhibition values obtained from the two previous assays are quite similar for all the compounds (see for comparison Table 2 where the decrease of ThT fluorescence intensity is expressed like in ThT assay in %) except for compounds **12e**, **12f**, and **13a** for which the values are significantly higher in the ThT fluorescence assay compared to ThT displacement assay, suggesting a greater inhibitory effect.

Table 2

% ThT fluorescence inhibition obtained by both the ThT fibrillation assay from the AcPHF6 peptide and the ThT displacement assay realized from preformed AcPHF6 fibers. The values (%) reported in the table are the mean values. For the ThT assay, these values are those reported in Fig. 2, for ThT displacement assay the values are calculated from the fluorescence emission intensities at 480 nm.

Indanone	ThT fluorescence inhibition (%)		Aurone	ThT fluorescence inhibition (%)	
	ThT fluorescence assay	ThT displacement assay		ThT fluorescence assay	ThT displacement assay
11e	-4	-10	**12e**	51	22
11f	5	6	**12f**	69	45
13a	71	42	**14a**	68	70
13b	83	78	**14b**	91	88
13m	72	76	**14m**	94	89
13n	78	65	**14n**	93	85
13o	87	90	**14o**	99	94

3.4. CD and AFM experiments.

The combination of fluorescence spectroscopy, circular dichroism (CD) spectroscopy and atomic force microscopy (AFM) was used to better characterize the interaction of compounds with AcPHF6 model.

CD spectroscopy provides structural information on β-sheet patterns. These β-sheets (from soluble oligomeric species or fibers) are expected to be detected during the fibrillation process, but are likely to disappear, or at least to decrease, when an inhibitor is added.

We selected a set of aurone/indanone pairs based on the results of the fluorescence experiments: the two **11e**/**12e** and **11f**/**12f** pairs where only the aurone analogue is active on both fluorescence assays; the **13a**/**14a** pair where both aurone and indanone are active on ThT assay but showing a different behavior in the ThT displacement test; and finally, the **13b**/**14b** and **13o**/**14o** pairs where all aurones and indanones are active on both fluorescence tests.

Among all the tested compounds, the CD profiles were significantly altered only in the presence of the indanones **13a**, **13b** and **13o** (Fig. 5). For the **11e**/**12e** and **11f**/**12f** pairs the CD profiles were the same for the active aurones and the corresponding inactive indanones (Fig. 5 and Fig. S4 for **11e**/**12e**). The aurones **12e** and **12f** were not able to inhibit the formation of β-sheet species suggesting that their effect can be mostly attributed to a displacement of the bound ThT from fibers. The other selected pairs had all the same behavior in CD. The indanones **13a**, **13b** and **13o** showed a significant inhibition of the β-sheet profile in CD whereas the aurones did not. This is not in contradiction with fluorescence assays but suggests that only the indanone derivatives have an inhibitory effect on AcPHF6 fibril formation. The effect of aurones seems to be mostly due to a ThT agonist effect.

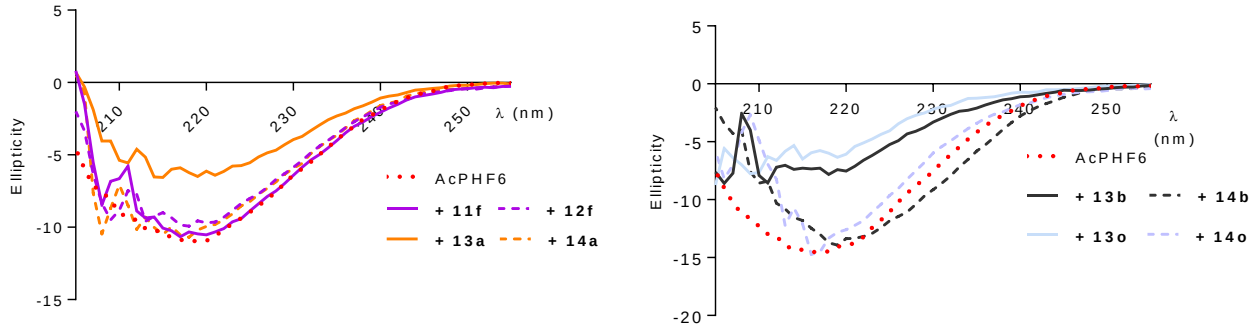

Fig. 5. CD spectra obtained after a 2 h incubation at room temperature of AcPHF6 at 100 µM in phosphate buffer 50 mM, alone or in presence of 100 µM of one of the compounds.

Lastly, compounds **13a**, **13b** and **13o** that have shown β-sheet inhibitory properties in DC were incubated with AcPHF6 for 24 h to obtain the AFM images depicted in figure 6. In the absence of inhibitors, AcPHF6 was able to create a tight fiber network (Fig. 6A). This fibrillation was largely inhibited in presence of 100 µM indanone **13a** (Fig. 6B) since only a few aggregates remained after 24 h. Contrariwise, the indanones **13b** (Fig. 6C) and **13o** (Fig. 6D) at the same 100 µM concentration did not inhibit the fibrillation of AcPHF6, although the fiber network was less dense, especially for **13o**. To conclude, compounds **13b** and **13o** were capable of reducing the amount of β-sheet fibers but are not able to stabilize aggregates, unlike compound **13a**. As a comparison, AFM images of the inactive aurone **14a**, the analogue of indanone **13a**, are reported in figure S6.

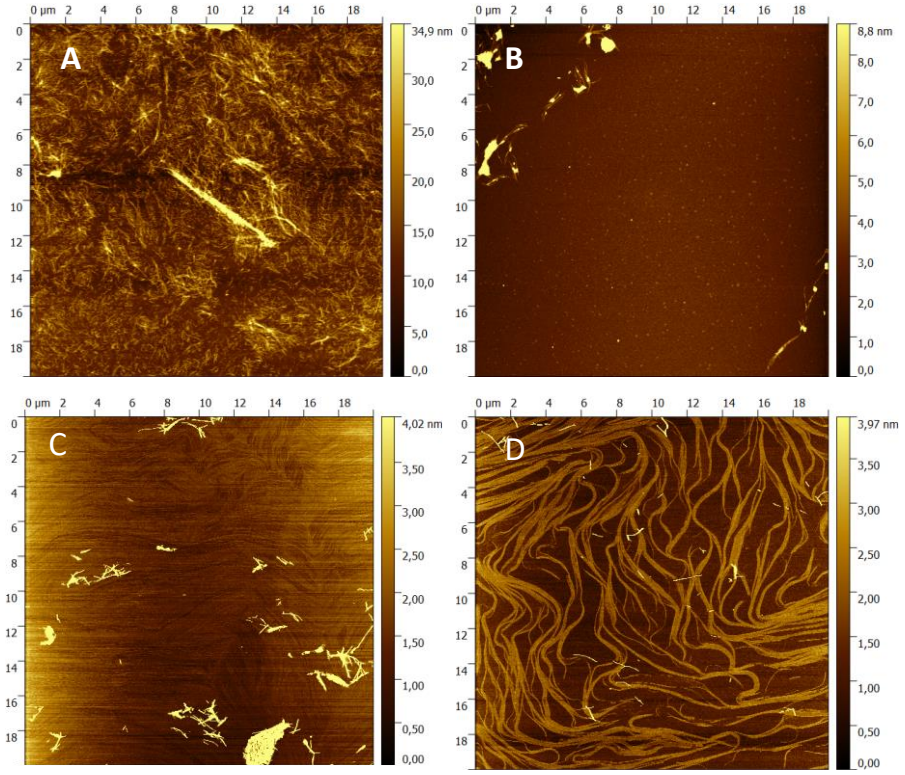

Fig. 6. AFM images obtained after 24 h of fibrillation of 100 µM AcPHF6 alone (A) or with 100 µM of **13a** (B), **13b** (C) and **13o** (D).

3.5. Molecular modelling.

To better understand the difference in the way these two families of compounds interact with their target, molecular modelling was used to compare the three-dimensional structure of aurone **14a** and indanone **13a** with myricetin, a known polyphenolic inhibitor of the tau fibers elongation (Fig. 7). Whereas the electronic density of the aurone and indanone analogues is quite similar, the spatial orientation of cycles A and B are substantially different. The three-dimensional shape of the indanone comes closer to that of myricetin with orthogonal cycles which can explain their common properties related to the inhibition of amyloid AcPHF6 fibers.

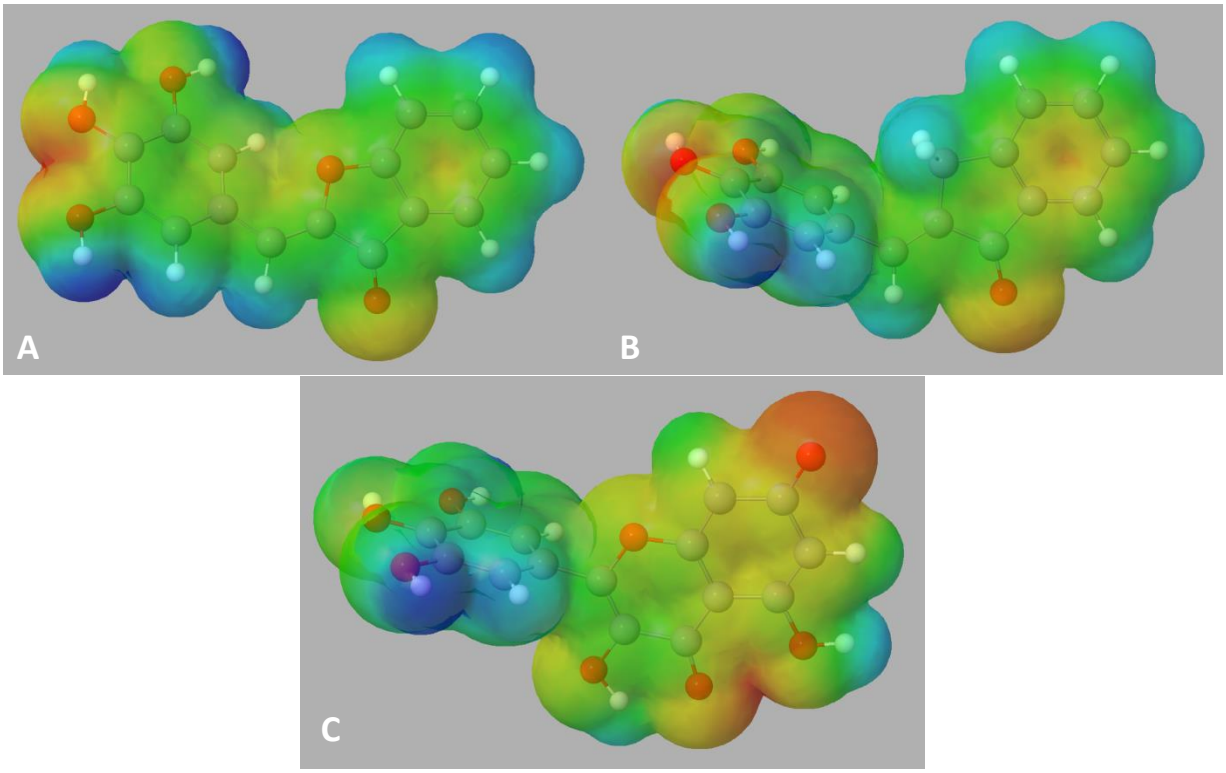

Fig. 7. Three-dimensional structure and electronic density of aurone **14a** (A), indanone **13a** (B) and myricetin (C).

4. Conclusion

In an effort to deepen the knowledge related to the activity of polyphenol derivatives on the aggregation of a tau model, AcPHF6, we have synthesized a set of aurone and indanone derivatives. The structure-activity relationship studies highlighted the significant effect of the number and the position of hydroxyl substituents on the synthesized analogues for the close interaction with AcPHF6. Moreover, the tridimensional geometry of the molecule was shown to play a potential role in determining if it acts as inhibitors of fiber elongation or as chemical probes of fibers. In short, indanones, which possess a conformation similar to myricetin, have been identified as relevant inhibitors when substituted at least by three hydroxyl groups. In addition, the preliminary kinetic assays carried out not on AcPHF6 model but directly on the tau protein have shown that the fibrillation inhibitory effect of indanones **13a**, **13b** and **13o** was also found on the full length protein. Further study would be needed, but this activity similar to that of myricetin is very promising (Fig. S5). Finally, considering the large other known activities of indanones on neurodegenerative process – notably as acetylcholinesterase inhibitors or as antioxidants, it would be of particular interest to evaluate these polyhydroxylated indanones in a multi-target strategy against AD.

5. Experimental section

5.1. Chemistry

Commercially available reagents and solvents were used without further purification. Reactions were monitored by thin-layer chromatography (plates coated with silica gel 60 F254 from Merck). Silica gel 60 (70-230 mesh from Macherey-Nagel) was used for flash chromatography. ^{1}H and ^{13}C NMR spectra were recorded at room temperature in deuterated solvents on a Brüker Avance 400 or Avance III 500 instrument (400 or 500 MHz). Chemical shifts (δ) are reported in parts per million (ppm) relative to TMS as internal standard or relative to solvent [^{1}H: δ(DMSO-*d6*) = 2.50 ppm, $\delta(CD_3OD)$ = 3.31 ppm, $\delta(CDCl_3)$ = 7.24 ppm; ^{13}C: δ(DMSO-*d6*) = 39.5 ppm, $\delta(CD_3OD)$ = 49.0 ppm, $\delta(CDCl_3)$ = 77.2 ppm]. Electrospray ionization ESI mass spectra were acquired on an Esquire 300 Plus Bruker Daltonis instrument with a nanospray inlet and accurate mass measurements (HRMS) were carried out on a TOF spectrometer, realized by the Analytical Department of Grenoble University. HPLC analyses were recorded on an Agilent 1100 series using a diode array detector and a C18 reversed-phase column (Nucleosil C18, Macherey-Nagel, 5 µm particle size, 125 mm × 3 mm) at 25 °C, with a mobile phase A composed of water and TFA 0.1% and a phase mobile B composed of MeOH and TFA 0.1% with a gradient 85:15 to 0:100 A:B over 10 min, 1 mL/min, 30 µL injection, detection at 254 nm. Purity of all the reported compounds was ≥ 95%.

*5.1.1. General procedure A for the synthesis of indanone compounds (**11a−o**)*

To a solution of an indanone (1 equiv.) in EtOH (5 mL/mmol) were added a benzaldehyde derivative (1 equiv.) and then dropwise an aqueous solution of NaOH 5% (2 equiv.). After stirring for 3 to 7 h at room temperature, the reaction mixture was cooled for 30 min in an ice bath. If necessary (presence of phenolic group), the reaction mixture was acidified by an aqueous solution of HCl (1 M). If a precipitation occurred, the mixture was filtered and washed with cold water and MeOH; if no precipitation was noticed, then the mixture was extracted 3 times with EtOAc and the organic layer was dried over $MgSO_4$, filtered and concentrated *in vacuo*. In the latter case, the residue was purified by flash chromatography on silica gel (CH_2Cl_2 to CH_2Cl_2/MeOH 95:5).

5.1.1.1. (E)-2-(3,4,5-trimethoxybenzylidene)-2,3-dihydro-1H-inden-1-one [27] ***(11a)**, (E)-2-benzylidene-2,3-dihydro-1H-inden-1-one* [28] ***(11c)**, (E)-2-(3-hydroxybenzylidene)-2,3-dihydro-1H-inden-1-one*[29] ***(11d)**, (E)-4-hydroxy-2-(3-hydroxybenzylidene)-2,3-dihydro-1H-inden-1-one* [29] ***(11f)**, (E)-2-(3,5-dimethoxybenzylidene)-2,3-dihydro-1H-inden-1-one* [30] ***(11g)**, (E)-2-benzylidene-5,7-dimethoxy-2,3-dihydro-1H-inden-1-one* [31] ***(11j)**, (E)-5,7-dimethoxy-2-(3-methoxybenzylidene)-2,3-dihydro-1H-inden-1-one* [31] ***(11k)**, (E)-2-(3,5-dimethoxybenzylidene)-5,7-dimethoxy-2,3-dihydro-1H-inden-1-one* [31] ***(11l)*** and *(E)-2-(3,4-dimethoxybenzylidene)-5,7-dimethoxy-2,3-dihydro-1H-inden-1-one* [31] ***(11n)*** were synthesized according to general

procedure A. Pure products were obtained with a yield of 94%, 75%, 62%, 36%, 73%, 73%, 81%, 24% and 73% respectively. Spectral data are in accordance with literature.

*5.1.1.2. (E)-4-hydroxy-2-(3,4,5-trimethoxybenzylidene)-2,3-dihydro-1H-inden-1-one (**11b**).* The crude product was prepared according to the general procedure A starting from **2** (100 mg, 0.68 mmol) and commercially available 3,4,5-trimethoxybenzaldehyde (133 mg, 0.68 mmol). The pure product (78 mg, 0.24 mmol, 35%) was obtained as a yellow solid. Rf 0.41 (cyclohexane/EtOAc/MeOH 70:20:10); ^{1}H NMR (400 MHz, DMSO-d_6) δ ppm 3.74 (s, 3H), 3.89 (s, 6H), 3.98 (bs, 2H), 7.09-7.14 (m, 3H), 7.23-7.27 (m, 1H), 7.29-7.34 (m, 1H), 7.49-7.51 (m, 1H), 10.03 (s, 1H); ^{13}C NMR (100 MHz, DMSO-d_6) δ ppm 28.7 (CH_2), 56.1 (2xCH_3), 60.2 (CH_3), 108.4 (2xCH), 114.2 (CH), 120.5 (CH), 129.1 (CH), 130.4 (CH), 133.3 (C), 134.0 (C), 136.1 (C), 138.9 (C), 139.2 (C), 153.0 (2xC), 154.7 (C), 193.5 (C); LRMS (ESI$^+$) *m/z* (%) 327 $[M+H]^+$ (100); HRMS (ESI$^+$) *m/z* calc. for $C_{19}H_{19}O_5$ 327.1232, found 327.1227.

*5.1.1.3. (E)-2-benzylidene-4-hydroxy-2,3-dihydro-1H-inden-1-one (**11e**).* The crude product was prepared according to the general procedure A starting from **2** (100 mg, 0.68 mmol) and commercially available benzaldehyde (72 mg, 0.68 mmol). The pure product (72 mg, 0.31 mmol, 45%) was obtained after washing with dichloromethane as a yellow solid. Rf 0.59 (cyclohexane/EtOAc/MeOH 50:30:20); ^{1}H NMR (400 MHz, DMSO-d_6) δ ppm 3.95 (bs, 2H), 7.11 (dd, *J* = 7.7, 1.0 Hz, 1H), 7.26 (dd, *J* = 7.5, 1.0 Hz, 1H), 7.29-7.35 (m, 1H), 7.45-7.49 (m, 1H), 7.50-7.56 (m, 3H) 7.81 (d, *J* = 7.3 Hz, 2H), 10.1 (s, 1H); ^{13}C NMR (100 MHz, DMSO-d_6) δ ppm 29.1 (CH_2), 114.1 (CH), 120.4 (CH), 129.0 (2xCH), 129.1 (CH), 129.8 (CH), 130.7 (2xCH), 132.8 (CH), 134.9 (C), 135.1 (C), 136.4 (C), 138.9 (C), 154.8 (C), 193.6 (C); LRMS (ESI$^-$) *m/z* (%) 235 $[M-H]^-$ (100); HRMS (ESI$^-$) *m/z* calc. for $C_{16}H_{11}O_2$ 235.0759, found 235.0754.

*5.1.1.4. (E)-2-(3,5-dimethoxybenzylidene)-4-hydroxy-2,3-dihydro-1H-inden-1-one (**11h**).* The crude product was prepared according to the general procedure A starting from **2** (100 mg, 0.68 mmol) and commercially available 3,5-dimethoxybenzaldehyde (113 mg, 0.68 mmol). The pure product (80 mg, 0.27 mmol, 40%) was obtained as a light brown solid. Rf 0.38 (cyclohexane/EtOAc/MeOH 70:20:10); ^{1}H NMR (400 MHz, DMSO-d_6) δ ppm 3.82 (s, 6H), 3.94 (bs, 2H), 6.62 (t, *J* = 2.2 Hz, 1H), 6.95 (d, *J* = 2.2 Hz, 2H), 7.10 (dd, *J* = 7.7, 1.0 Hz, 1H), 7.25 (dd, *J* = 7.4, 0.8 Hz, 1H), 7.29-7.34 (m, 1H), 7.44-7.47 (m, 1H), 10.06 (s, 1H); ^{13}C NMR (100 MHz, DMSO-d_6) δ ppm 29.0 (CH_2), 55.4 (2xCH_3), 101.8 (CH), 108.7 (2xCH), 114.2 (CH), 120.6 (CH), 129.1 (CH), 132.9 (CH), 135.5 (C), 136.2 (C), 136.7 (C), 138.8 (C), 154.8 (2xC), 160.7 (C), 193.6 (C); LRMS (ESI$^-$) *m/z* (%) 295 $[M-H]^-$ (100); HRMS (ESI$^-$) *m/z* calc. for $C_{18}H_{15}O_4$ 295.0970, found 295.0974.

*5.1.1.5. (E)-2-(2,3,4-trimethoxybenzylidene)-4-hydroxy-2,3-dihydro-(1H)-inden-1-one (**11i**).* The crude product was prepared according to the general procedure A starting from **2** (200 mg, 1.35

mmol) and 2,3,4-trimethoxybenzaldehyde (265 mg, 1.35 mmol). The pure product (335 mg, 1.03 mmol, 76%) was obtained as a grey powder. Rf 0.19 (CH_2Cl_2/MeOH 99:1); ^{1}H NMR (400 MHz, DMSO-d_6) δ ppm 3.78 (s, 3H), 3.82-3.93 (m, 8H), 6.98 (d, J = 8.9 Hz, 1H), 7.09 (d, J = 7.5 Hz, 1H), 7.23 (d, J = 7.5 Hz, 1H), 7.30 (dd, J = 7.5, 7.5 Hz, 1H), 7.58 (d, J = 8.9 Hz, 1H), 7.74 (s, 1H), 10.08 (bs, 1H, OH); ^{13}C NMR (100 MHz, DMSO-d_6) δ ppm 29.0 (CH_2), 56.1 (CH_3), 60.5 (CH_3), 61.7 (CH_3), 108.4 (CH), 114.1 (CH), 120.2 (CH), 121.4 (C), 124.9 (CH), 126.7 (CH), 129.0 (CH), 133.5 (C), 136.2 (C), 139.1 (C), 141.9 (C), 153.7 (C), 154.8 (C), 155.3 (C), 193.5 (C); LRMS (ESI+) *m/z* (%) 327 (100) $[M+H]^+$, 349 (40) $[M+Na]^+$; HRMS (ESI+) *m/z* calc. for $C_{19}H_{16}O_5$ 327.1227, found 327.1220.

*5.1.1.6. (E)-2-(2,4-dimethoxybenzylidene)-5,7-dimethoxy-2,3-dihydro-1H-inden-1-one (**11m**).* The crude product was prepared according to the general procedure A starting from **6** (80 mg, 0.42 mmol) and 2,4-dimethoxybenzaldehyde (69 mg, 0.42 mmol). The purity of the product was checked by TLC, not by NMR due to insolubility. The pure product (65 mg, 0.19 mmol, 46%) was obtained as a yellowish powder. Rf 0.20 (CH_2Cl_2/MeOH 99:1); LRMS (ESI^+) *m/z* (%) 341 (100) $[M+H]^+$; HRMS (ESI^+) *m/z* calc. for $C_{20}H_{21}O_5$ 341.1389, found 341.1394.

*5.1.1.7. (E)-5,7-dimethoxy-2-(3,4,5-trimethoxybenzylidene)-2,3-dihydro-1H-inden-1-one (**11o**).* The crude product was prepared according to the general procedure A starting from **6** (110 mg, 0.58 mmol) and commercially available 3,4,5-trimethoxybenzaldehyde (114 mg, 0.58 mmol). The pure product (60 mg, 0.16 mmol, 28%) was obtained as a yellow solid. Rf 0.47 (cyclohexane/EtOAc/MeOH 50:30:20); ^{1}H NMR (400 MHz, DMSO-d_6) δ ppm 3.71 (s, 3H), 3.87 (s, 9H), 3.89 (s, 3H), 4.05 (bs, 2H), 6.51 (d, J = 1.8 Hz, 1H), 6.71 (d, J = 1.8 Hz, 1H), 7.04 (s, 2H), 7.27-7.30 (m, 1H); ^{13}C NMR (100 MHz, DMSO-d_6) δ ppm 31.7 (CH_2), 55.6 (CH_3), 55.9 (CH_3), 56,0 (2xCH_3), 60.1 (CH_3), 97.7 (CH), 102.1 (CH), 107.9 (2xCH), 119.5 (C), 130.3 (CH), 130.7 (C), 135.1 (C), 138.6 (C), 153.0 (2xC), 154.5 (C), 159.6 (C), 166.5 (C), 189.1 (C); LRMS (ESI^+) *m/z* (%) 371 $[M+H]^+$ (100); HRMS (ESI^+) *m/z* calc. for $C_{21}H_{23}O_6$ 371.1495, found 371.1493.

*5.1.2. General procedure B1 for the synthesis of aurone derivatives (**12a-c, e-f, i, l-o**)*

To a solution of a benzofuran-3(2*H*)-one derivative in dry dichloromethane (20 mL/mmol) were added a benzaldehyde derivative (1.2 to 1.5 equiv.) and aluminium oxide (4.0 g/mmol). The suspension was stirred at room temperature under nitrogen overnight, then filtered and concentrated *in vacuo*. The product was recrystallized in MeOH and filtered off to afford the corresponding pure aurone derivative.

5.1.2.1. (Z)-2-[(3,4,5-trimethoxy)phenylmethylene]benzofuran-3(2H)-one [32] *(**12a**), (Z)-7-methoxy-2-(3,4,5-trimethoxybenzylidene)benzofuran-3(2H)-one* [11] *(**12b**), (Z)-2-benzylidenebenzofuran-3(2H)-one* [31] *(**12c**), (Z)-2-benzylidene-7-methoxybenzofuran-3(2H)-one* [11] *(**12e**), (Z)-7-*

methoxy-2-(3-methoxybenzylidene)benzofuran-3(2H)-one [11] ***(12f)***, *(Z)-7-methoxy-2-(2,3,4-trimethoxybenzylidene)benzofuran-3(2H)-one* [11] ***(12i)***, *(Z)-2-(3,5-dihydroxybenzylidene)-4,6-dihydroxybenzofuran-3(2H)-one* [33] ***(12l)***, *(Z)-2-(2,4-dimethoxybenzylidene)-4,6-dimethoxybenzofuran-3(2H)-one* [34] ***(12m)***, *(Z)-2-(3,4-dimethoxybenzylidene)-4,6-dimethoxybenzofuran-3(2H)-one* [33] ***(12n)*** and *(Z)-2-(3,4,5-trimethoxybenzylidene)-4,6-dimethoxy-benzofuran-3(2H)-one* [35] ***(12o)*** were synthesized according to general procedure B1. Pure products were obtained with a yield of 85%, 79%, 78%, 65%, 77%, 74%, 6%, 91%, 80% and 92% respectively. Spectral data are in accordance with literature.

*5.1.3. (Z)-2-(3,5-dihydroxybenzylidene)-4,6-dihydroxybenzofuran-3(2H)-one (**12g**).* The synthesis and spectral data were described in Lunven *et al* [11].

*5.1.4. General procedure B2 for the synthesis of aurone derivatives (**12j-k**)*

4,6-dihydroxybenzofuran-3(2*H*)-one (1 equiv.) was dissolved in MeOH (15 mL/mmol). An aqueous solution of potassium hydroxide (50%, 1.5 mL/mmol) and a benzaldehyde derivative (1.5 equiv.) were added to the mixture which was stirred at 70 °C in the microwave reactor for 2 to 10 h and concentrated under reduced pressure. The reaction mixture was diluted with water and acidified with 1 M HCl until pH 2-3, then extracted with EtOAc. The combined organic layers were washed with water and brine, filtered and dried over $MgSO_4$. Filtration and concentration *in vacuo* gave the corresponding crude aurone derivative. This residue was purified by flash chromatography on silica gel (CH_2Cl_2 to CH_2Cl_2/MeOH 95:5).

5.1.4.1. (Z)-2-benzylidene-4,6-dihydroxybenzofuran-3(2H)-one [34] ***(12j)*** and *(Z)-4,6-dihydroxy-2-(3-hydroxybenzylidene)benzofuran-3(2H)-one* [36] ***(12k)*** were synthesized according to general procedure B2. Pure products were obtained with a yield of 82% and 50% respectively. Spectral data are in accordance with literature.

*5.1.5. General procedure C for the deprotection of the methoxylated indanone / aurone derivatives (**13a-b, g-o** and **14a-b, i, m-o**)*

To a solution of a methoxylated indanone or aurone derivatives (1 equiv.) in dry dichloromethane (10 mL/mmol) was added BBr_3 (20 equiv.) at 0 °C. After stirring at room temperature and under N_2 atmosphere for 24 to 72 h (until TLC showed total consumption of starting material), cold water was added and the mixture was extracted 3 times with EtOAc. The organic layer was dried over $MgSO_4$, filtered and concentrated *in vacuo*. The compounds obtained were pure enough to avoid any purification.

*5.1.5.1. (E)-2-(3,4,5-trihydroxybenzylidene)-2,3-dihydro-1H-inden-1-one (**13a**).* The crude product was prepared according to the general procedure C starting from **11a** (70 mg, 0.23 mmol). The

pure product (18 mg, 0.07 mmol, 30%) was obtained as a brown solid. Rf 0.47 (cyclohexane/EtOAc/MeOH 50:30:20); ^{1}H NMR (400 MHz, DMSO-*d*$_6$) *δ* ppm 4.00 (bs, 2H), 6.77 (s, 2H), 7.29 (t, *J* = 1.8 Hz, 1H), 7.44-7.50 (m, 1H), 7.64-7.72 (m, 2H), 7.74-7.78 (m, 2H); ^{13}C NMR (100 MHz, DMSO-*d*$_6$) *δ* ppm 32.0 (CH_2), 110.5 (2xCH), 123.4 (CH), 125.2 (CH), 126.6 (CH), 127.6 (CH), 131.4 (CH), 134,2 (C), 134.4 (C), 136.3 (C), 137.7 (C), 146.2 (2xC), 149.6 (C), 193.1 (C); LRMS (ESI$^+$) *m/z* (%) 269 $[M+H]^+$ (100); HRMS (ESI$^-$) *m/z* calc. for $C_{16}H_{11}O_4$ 267.0656, found 267.0663.

*5.1.5.2. (E)-4-hydroxy-2-(3,4,5-trihydroxybenzylidene)-2,3-dihydro-1H-inden-1-one (**13b**).* The crude product was prepared according to the general procedure C starting from **11b** (48 mg, 0.15 mmol). The pure product (35 mg, 0.12 mmol, 83%) was obtained as a brown solid. Rf 0.31 (cyclohexane/EtOAc/MeOH 50:30:20); ^{1}H NMR (400 MHz, DMSO-*d*$_6$) *δ* ppm 3.81 (bs, 2H), 6.78 (s, 2H), 7.08 (d, *J* = 7.8 Hz, 1H), 7.21 (d, *J* = 7.2 Hz, 1H), 7.24-7.31 (m, 2H); ^{13}C NMR (100 MHz, DMSO-*d*$_6$) *δ* ppm 29.2 (CH_2), 110.4 (2xCH), 113.9 (CH), 119.9 (CH), 125.2 (CH), 128.9 (CH), 131.4 (C), 134.1 (C), 136.0 (C), 136.2 (C), 139.3 (C), 146.2 (2xC), 154.7 (C), 193.4 (C); LRMS (ESI$^-$) *m/z* (%) 283 $[M-H]^-$ (100); HRMS (ESI$^-$) *m/z* calc. for $C_{16}H_{11}O_4$ 267.0656, found 267.0657.

*5.1.5.3. (E)-2-(3,5-dihydroxybenzylidene)-2,3-dihydro-1H-inden-1-one (**13g**).* The crude product was prepared according to the general procedure C starting from **11g** (100 mg, 0.36 mmol). The pure product (67 mg, 0.26 mmol, 74%) was obtained as a brown solid. Rf 0.55 (cyclohexane/EtOAc/MeOH 50:30:20); ^{1}H NMR (400 MHz, DMSO-*d*$_6$) *δ* ppm 4.05 (bs, 2H), 6.33 (t, *J* = 2.0 Hz, 1H), 6.64 (d, *J* = 2.0 Hz, 2H), 7.32 (t, *J* = 1.9 Hz, 1H), 7.45-7.52 (m, 1H), 7.65-7.75 (m, *2*H), 7.76-7.78 (m, 1H); ^{13}C NMR (100 MHz, DMSO-*d*$_6$) *δ* ppm 32.0 (CH_2), 104.5 (CH), 108.9 (2xCH), 123.5 (CH), 126.7 (CH), 127.7 (CH), 133.4 (C), 134.6 (C), 134.9 (C), 136.3 (C), 137.2 (C), 149.9 (C), 158.7 (2xC), 193.4 (C); LRMS (ESI$^+$) *m/z* (%) 253 $[M+H]^+$ (100); HRMS (ESI$^-$) *m/z* calc. for $C_{16}H_{11}O_3$ 251.0709, found 251.0713.

*5.1.5.4. (E)-2-(3,5-dihydroxybenzylidene)-4-hydroxy-2,3-dihydro-1H-inden-1-one (**13h**).* The crude product was prepared according to the general procedure C starting from **11h** (50 mg, 0.17 mmol). The pure product (46 mg, 0.17 mmol, 100%) was obtained as a brown solid. Rf 0.44 (cyclohexane/EtOAc/MeOH 50:30:20); ^{1}H NMR (400 MHz, DMSO-*d*$_6$) *δ* ppm 3.85 (bs, 2H), 6.32 (t, *J* = 2.0 Hz, 1H), 6.65 (d, *J* = 2.0 Hz, 2H), 7.07-7.12 (m, 1H), 7.21-7.25 (m, 1H), 7.27-7.33 (m, 2H), 9.53 (s, 2H), 10.14 (s, 1H); ^{13}C NMR (100 MHz, DMSO-*d*$_6$) *δ* ppm 29.2 (CH_2), 104.4 (CH), 108.9 (2xCH), 114.1 (CH), 120.3 (CH), 129.0 (CH), 133.4 (C), 134.6 (CH), 136,3 (C), 136.4 (C), 138.9 (C), 154.8 (C), 158.7 (2xC), 193.6 (C); LRMS (ESI$^-$) *m/z* (%) 267 $[M-H]^-$ (100); HRMS (ESI$^-$) *m/z* calc. for $C_{16}H_{11}O_4$ 267.0656, found 267.0657.

*5.1.5.5. (E)-2-(2,3,4-trihydroxybenzylidene)-4-hydroxy-2,3-dihydro-1H-inden-1-one (**13i**).* The crude product was prepared according to the general procedure C starting from **11i** (100 mg, 0.31 mmol). The pure product (72 mg, 0.25 mmol, 83%) was obtained as a brown powder. Rf 0.44 (CH_2Cl_2/MeOH 9:1); ^{1}H NMR (400 MHz, CD_3OD) δ ppm 3.86 (d, *J* = 1.4 Hz, 2H), 6.49 (d, *J* = 8.7 Hz, 1H), 7.04 (d, *J* = 7.6, 1.0 Hz, 1H), 7.23 (d, *J* = 8.7 Hz, 1H), 7.27 (dd, *J* = 7.6, 7.5 Hz, 1H), 7.32 (dd, *J* = 7.5, 1.0 Hz, 1H), 8.15 (t, *J* = 1.4 Hz, 1H); ^{13}C NMR (100 MHz, CD_3OD) δ ppm 30.4 (CH_2), 108.8 (CH), 115.7 (CH), 116.5 (C), 121.1 (CH), 122.3 (CH), 130.0 (CH), 131.5 (CH), 131.8 (C), 134.2 (C), 137.9 (C), 141.0 (C), 149.4 (C), 150.1 (C), 155.9 (C), 197.2 (C); LRMS (ESI$^-$) *m/z* (%) 283 (100) [M-H]$^-$, 319 (20) [M+Cl]$^-$; HRMS (ESI$^-$) *m/z* calc. for $C_{16}H_{11}O_5$ 283.0601, found 283.0615.

*5.1.5.6. (E)-2-benzylidene-5,7-dihydroxy-2,3-dihydro-1H-inden-1-one (**13j**).* The crude product was prepared according to the general procedure C starting from **11j** (27 mg, 0.10 mmol). The pure product (24 mg, 0.10 mmol, 100%) was obtained as a yellow solid. Rf 0.38 (cyclohexane/EtOAc/MeOH 60:30:10); ^{1}H NMR (400 MHz, DMSO-d_6) δ ppm 3.94 (s, 2H), 6.21 (d, *J* = 1.8 Hz, 1H), 6.44 (d, *J* = 1.8 Hz, 1H), 7.29-7.33 (m, 1H), 7.39-7.44 (m, 1H), 7.45-7.51 (m, 2H), 7.72 (d, *J* = 7.3 Hz, 2H), 9.97 (s, 1H), 10.50 (s, 1H); ^{13}C NMR (100 MHz, DMSO-d_6) δ ppm 31.8 (CH_2), 101.1 (CH), 104.3 (CH), 117.1 (CH), 128.9 (2xCH), 129.2 (C), 129.6 (CH), 130.3 (2xCH), 135.2 (C), 136.4 (C), 153.2 (C), 158.8 (C), 165.7 (C), 190.7 (C); LRMS (ESI$^-$) *m/z* (%) 251 [M-H]$^-$ (100); HRMS (ESI$^-$) *m/z* calc. for $C_{16}H_{11}O_3$ 251.0709, found 251.0706.

*5.1.5.7. (E)-5,7-dihydroxy-2-(3-hydroxybenzylidene)-2,3-dihydro-1H-inden-1-one (**13k**).* The crude product was prepared according to the general procedure C starting from **11k** (31 mg, 0.10 mmol). The pure product (27 mg, 0.10 mmol, 100%) was obtained as a yellow solid. Rf 0.45 (cyclohexane/EtOAc/MeOH 40:50:10); ^{1}H NMR (400 MHz, DMSO-d_6) δ ppm 3.89 (s, 2H), 6.21 (d, *J* = 1.8 Hz, 1H), 6.43 (d, *J* = 1.8 Hz, 1H), 6.82 (m, 1H), 7.07-7.16 (m, 2H), 7.18-7.23 (m, 1H), 7.24-7.31 (m, 1H), 9.60 (s, 1H), 9.95 (s, 1H), 10.50 (s, 1H); ^{13}C NMR (100 MHz, DMSO-d_6) δ ppm 31.9 (CH_2), 101.1 (CH), 104.3 (CH), 116.5 (CH), 116.6 (CH), 117.1 (CH), 121.6 (C), 129.9 (2xCH), 136.1 (C), 136.4 (C), 153.1 (C), 157.6 (C), 158.8 (C), 165.6 (C), 190.8 (C); LRMS (ESI$^-$) *m/z* (%) 267 [M-H]$^-$ (100); HRMS (ESI$^-$) *m/z* calc. for $C_{16}H_{11}O_4$ 267.0657, found 267.0656.

*5.1.5.8. (E)-2-(3,5-dihydroxybenzylidene)-5,7-dihydroxy-2,3-dihydro-1H-inden-1-one (**13l**).* The crude product was prepared according to the general procedure C starting from **11l** (41 mg, 0.12 mmol). The pure product (14 mg, 0.05 mmol, 41%) was obtained as a brown solid. Rf 0.39 (cyclohexane/EtOAc/MeOH 50:30:20); ^{1}H NMR (400 MHz, DMSO-d_6) δ ppm 3.84 (s, 2H), 6.20 (d, *J* = 1.8 Hz, 1H), 6.28 (t, *J* = 2.1 Hz, 1H), 6.42 (d, *J* = 1.8 Hz, 1H), 6.55 (d, *J* = 2.1 Hz, 2H), 7.06-7.10 (m, 1H), 9.43 (s, 2H), 9.93 (s, 1H), 10.49 (s, 1H); ^{13}C NMR (125 MHz, DMSO-d_6) δ ppm 31.9 (CH_2), 101.1 (CH), 103.8 (CH), 104.3 (CH), 108.5 (2xCH), 117.2 (C), 130.3 (CH), 135.8 (C), 136.7

(C), 153.0 (C), 158.6 (2xC), 158.7 (C), 165.6 (C), 190.8 (C); LRMS (ESI^-) *m/z* (%) 283 $[M-H]^-$ (100); HRMS (ESI^+) *m/z* calc. for $C_{16}H_{13}O_5$ 285.0763, found 285.0760.

*5.1.5.9. (E)-2-(2,4-dihydroxybenzylidene)-5,7-dimethoxy-2,3-dihydro-1H-inden-1-one (**13m**).* The crude product was prepared according to the general procedure C starting from **11m** (45 mg, 0.13 mmol). After purification by column chromatography on silica gel (CH_2Cl_2 to CH_2Cl_2/MeOH 9:1), the pure product (20 mg, 0.07 mmol, 53%) was obtained as a yellow powder. Rf 0.49 (CH_2Cl_2/MeOH 9:1); ^1H NMR (500 MHz, CD_3OD) δ ppm 3.85 (s, 2H), 6.17 (d, *J* = 1.5 Hz, 1H), 6.36 (d, *J* = 2.3 Hz, 1H), 6.40 (dd, *J* = 8.6, 2.3 Hz, 1H), 6.47 (d, *J* = 1.5 Hz, 1H), 7.54 (d, *J* = 8.6 Hz, 1H), 7.94 (s, 1H); ^{13}C NMR (125 MHz, CD_3OD) δ ppm 33.6 (CH_2), 101.5 (CH), 103.4 (CH), 105.6 (CH), 108.8 (CH), 115.8 (C), 118.7 (C), 128.5 (CH), 131.9 (C), 132.1 (CH), 154.0 (C), 160.9 (C), 160.9 (C), 162.1 (C), 167.7 (C), 196.3 (C); LRMS (ESI^-) *m/z* (%) 283 (100) $[M-H]^-$; HRMS (ESI^+) *m/z* calc. for $C_{16}H_{13}O_5$ 285.0763, found 285.0765.

*5.1.5.10. (E)-2-(3,4-dihydroxybenzylidene)-5,7-dihydroxy-2,3-dihydro-1H-inden-1-one (**13n**).* The crude product was prepared according to the general procedure C starting from **11n** (77 mg, 0.23 mmol). The pure product (58 mg, 0.20 mmol, 90%) was obtained as a brown powder. Rf 0.60 (CH_2Cl_2/MeOH 9:1); ^1H NMR (500 MHz, DMSO-d_6) δ ppm 3.83 (s, 2H), 6.19 (d, *J* = 1.6 Hz, 1H), 6.43 (d, *J* = 1.6 Hz, 1H), 6.83 (d, *J* = 8.3 Hz, 1H), 7.03 (dd, *J* = 8.3, 1.8 Hz, 1H), 7.14 (d, *J* = 1.8 Hz, 1H), 7.16 (s, 1H), 9.18 (s, 1H, OH), 9.54 (s, 1H, OH), 9.84 (s, 1H, OH), 10.45 (s, 1H, OH); ^{13}C NMR (125 MHz, DMSO-d_6) δ ppm 32.0 (CH_2), 100.9 (CH), 104.3 (CH), 116.0 (CH), 117.2 (CH), 123.6 (CH), 126.7 (C), 130.7 (CH), 132.4 (C), 145.5 (C), 147.4 (C), 152.7 (C), 158.6 (C), 165.4 (C), 191.3 (C); LRMS (ESI^-) *m/z* (%) 283 (100) $[M-H]^-$; HRMS (ESI^-) *m/z* calc. for $C_{16}H_{11}O_5$ 283.0601, found 283.0615.

*5.1.5.11. 2,3-dihydro-5,7-dihydroxy-2-[(3,4,5-trihydroxyphenyl) methylene]-1H-inden-1-one (**13o**).* The crude product was prepared according to the general procedure C starting from **11o** (45 mg, 0.12 mmol). The pure product (36 mg, 0.12 mmol, 100%) was obtained as an orange solid. Rf 0.29 (cyclohexane/EtOAc/MeOH 50:30:20); ^1H NMR (500 MHz, DMSO-d_6) δ ppm 3.80 (s, 2H), 6.19 (d, *J* = 1.7 Hz, 1H), 6.41-6.45 (m, 1H), 6.67 (s, 2H), 7.04-7.07 (m, 1H), 8.76 (bs, 1H), 9.11 (bs, 2H), 9.84 (bs, 1H), 10.45 (s, 1H); ^{13}C NMR (125 MHz, DMSO-d_6) δ ppm 32.0 (CH_2), 100.9 (CH), 104.3 (CH), 110.0 (2xCH), 117.2 (C), 125.5 (C), 131.2 (CH), 132.4 (C), 135.6 (C), 146.1 (2xC), 152.6 (C), 158.6 (C), 165.4 (C), 191.3 (C); LRMS (ESI^-) *m/z* (%) 299 $[M-H]^-$ (100); HRMS (ESI^+) *m/z* calc. for $C_{16}H_{13}O_6$ 301.0712, found 301.0713.

*5.1.5.12. (Z)-2-[(3,4,5-trihydroxy)phenylmethylene]benzofuran-3(2H)-one (**14a**).* The crude product was prepared according to the general procedure C starting from **12a** (70 mg, 0.22 mmol). The pure product (60 mg, 0.22 mmol, quantitative) was obtained as a brown powder. Rf 0.12

(CH_2Cl_2/MeOH 97:3); ^{1}H NMR (400 MHz, CD_3OD) δ ppm 6.74 (s, 1H), 7.06 (s, 2H), 7.27 (dd, *J* = 7.5, 7.5 Hz, 1H), 7.40 (d, *J* = 8.3 Hz, 1H), 7.74 (dd, *J* = 8.3, 7.5 Hz, 1H), 7.77 (d, *J* = 7.5 Hz, 1H); ^{13}C NMR (100 MHz, CD_3OD) δ ppm 112.6 (2xCH), 113.9 (CH), 116.7 (CH), 122.9 (C), 124.2 (C), 124.6 (CH), 125.2 (CH), 138.2 (C), 146.8 (C), 147.1 (2xC), 167.1 (C), 185.9 (C); LRMS (ESI^-) *m/z* (%) 269 (100) $[M-H]^-$; HRMS (ESI^-) *m/z* calc. for $C_{15}H_9O_5$ 269.0445, found 269.0459.

5.1.5.13. (Z)-7-hydroxy-2-(3,4,5-trihydroxybenzylidene)benzofuran-3(2H)-one [11] ***(14b)**, (Z)-7-hydroxy-2-(2,3,4-trihydroxybenzylidene)benzofuran-3(2H)-one* [11] ***(14i)**, (Z)-2-(2,4-dihydroxybenzylidene)-4,6-dihydroxybenzofuran-3(2H)-one* [34] ***(14m)*** and *(Z)-2-(3,4-dihydroxybenzylidene)-4,6-dihydroxybenzofuran-3(2H)-one* [34] ***(14n)*** were synthesized according to general procedure B1. Pure products were obtained with a yield of 39%, 60%, 63% and 65% respectively. Spectral data are in accordance with literature.

*5.1.5.14. (Z)-4,6-dihydroxy-2-(3,4,5-trihydroxybenzylidene)benzofuran-3(2H)-one (**14o**).* The crude product was prepared according to the general procedure C starting from **12o** (100 mg, 0.27 mmol). The pure product (54 mg, 0.18 mmol, 66%) was obtained after a flash chromatography on silica gel (CH_2Cl_2 to CH_2Cl_2/MeOH 8:2) as a brown powder. Rf 0.54 (CH_2Cl_2/MeOH 8:2); ^{1}H NMR (400 MHz, CD_3OD) δ ppm 6.03 (d, 1H, *J* = 1.6 Hz), 6.20 (d, 1H, *J* = 1.6 Hz), 6.49 (s, 1H), 6.97 (s, 2H); ^{13}C NMR (100 MHz, CD_3OD) δ ppm 91.6 (CH), 98.5 (CH), 104.7 (C), 111.9 (2xCH), 113.1 (CH), 124.6 (C), 137.2 (C), 147.0 (2xC), 148.0 (C), 159.9 (C), 169.5 (C), 169.6 (C), 182.8 (C); HRMS (ESI^+) *m/z* calc. for $C_{15}H_{11}O_7$ 303.0505, found 303.0505.

5.1.6. Peptide synthesis and purification

Ac-PHF6-NH_2 (AcPHF6, MW=1018 g/mol) were synthesized as previously reported.[11] Peptides were purified with a reverse-phase high pressure liquid chromatography (RP-HPLC) on a Nucleosil C18 column (100 Ă, 250 × 21 nm, 7 µM) with UV monitoring at 214 and 250 nm. During 25 min a 22 mL/min flow with a 15-35% acetonitrile in water was applied (both water and acetonitrile contained 0.1% TFA). Purified peptides were lyophilized, controlled by high resolution mass spectroscopy (HRMS, ESI+) and stored at -20 °C.

5.2. Biochemistry

5.2.1. Absorption spectra

Absorption spectra were acquired on a spectrophotometer SAFAS UVmc (SAFAS S.A, Monaco, France) with an optical length of 8.5 mm and a ray of 0.5 × 4 mm. Spectra were recorded using the software SAFAS SP2000 from 240 nm to 640 nm with a spectral resolution of 1 nm and an average time 0.3 s per data point from a drop of sample (5 µL). Final concentration of samples was 10 µM aurone or indanone in 50 mM phosphate buffer with a 0.5% maximum of DMSO.

5.2.2. Emission spectra

Emission spectra were acquired with a Perkin Elmer Luminescence Spectrometer LS50 using a quartz cell with a 0.3 cm path length and with a sample volume of 100 µL. Data were recorded using FL WinLab software from 300 to 600 nm with an excitation wavelength of 440 nm, and a scan speed of 150 nm/min. Emission spectra were recorded in 50 mM phosphate buffer with a maximum of 0.5% of DMSO (i) from 10 µM aurone or indanone, (ii) from a solution containing 10 µM aurone or indanone in presence of 100 µM of AcPHF6 fibers or (iii) from a solution of 10 µM aurone or indanone in presence of 100 µM AcPHF6 fibers prepared in presence of 10 µM ThT. Those AcPHF6 fibers were pre-formed with AcPHF6 1mM left 24 hours in deionised water, then 10 µL of AcPHF6 fibers were added to final solutions (ii and iii). Emission spectra were collected shortly after this AcPHF6 fibers addition.

5.2.3. Thioflavin T fluorescence assays

The kinetic of fibrillation was performed in 96-well black U-shape polypropylene microplate (Greiner Bio-One) in a POLARstar Omega fluorescence plate reader (BMG LABTECH GmbH, Offenburg, Germany). All conditions were tested in hexaplicate whose average represents the results given in this work.

5.2.3.1. AcPHF6 model. AcPHF6 peptide stock solution was dissolved, just before its addition into the plate, in water to a final concentration of 500 µM. In each well (final volume 100 µL) is added: 50 µL of 100 mM phosphate buffer, 10 µL of 100 µM ThT (10 µM final), 10 µL of pure water, 10 µL of 100 µM or 10 µM of the tested compound (10 or 1 µM final with less than 0.2% of DMSO) and 20 µL of 500 µM AcPHF6 peptide stock solution (100 µM final). Aurone-Indanone control wells were prepared under the same conditions with the exception of adding 20 µL of 100 mM phosphate buffer (50 mM final) containing 5% DMSO instead of AcPHF6 peptide.

5.2.3.2. Measurements. Fluorescence data was acquired every minute over two hours under an excitation and emission wavelengths at 440 and 480 nm, respectively. Reading (top optic, orbital averaging of 3mm diameter) was done with a 1200 gain. All results for 10 and 1 µM aurones-indanones final concentrations are reported in the figure 2.

5.2.4. Circular dichroism

Samples (200 µL final) were prepared in low-binding tubes for a final concentration of 100 µM AcPHF6, 10 µM aurone/indanone with less than 0.2% of DMSO in 50 mM phosphate buffer, and then directly transferred into a 300 µL quartz CD cell with a 1 mm path length. CD spectra were acquired on a JASCO J-810 spectropolarimeter (Jasco corporation, Tokyo, Japan). Data was recorded at room temperature between 260 to 190 nm with a spectral resolution of 1 nm, an average time of 1 s second per data point and a bandwidth of 10 nm.

5.2.5. Atomic force microscopy. AFM samples were collected from CD's samples after 24 h of incubation in room temperature for APHF6. A 5 µL drop from each sample was absorbed onto mica surface during 10 min then it was washed two-three times by 10 µL of pure water and subsequently removing it. AFM images (40 × 40 down to 0.5 × 0.5 µm2, 512 × 512 pixel) were recorded at randomly selected surface position in peak force mode using a Dimension Icon (Bruker, Santa Barbara, CA). The cantilevers SCANASYST-Air used were triangular and had a force contact of 0.4 N/m and a resonance frequency of 70 kHz at tip scan rates of 1 Hz. AFM was processed using the flattening function of the Gwyddion microscope software.

5.3. Molecular Modeling

Compound molecular structures were built with maestro and Ligprep modules from Schrödinger suite [37]. Geometries where further optimized with MOPAC2016 semi-empirical package using PM7 parameterization [38,39]. PULAY and PRECISE options where activated. Electronic densities were exported using GRAPH POTWRT keywords and mapped on respective molecular surfaces by JMol [40].

Acknowledgements

This work has been partially supported by Labex Arcane and CBH-EUR-GS (ANR-17-EURE-0003) and by NeuroCoG IDEX UGA in the framework of the "Investissements d'avenir" program (ANR-15-IDEX-02). The NanoBio ICMG platforms (FR 2607) are acknowledged for providing facilities for mass spectrometry analyses (A. Durand, L. Fort, R. Gueret) and for NMR analyses (M.-C. Molina).

Appendix A. Supplementary data

Supplementary data (^{1}H and ^{13}C NMR spectra) related to this article can be found at http://dx.doi.org/

References

[1] K. Iqbal, F. Liu, C.-X. Gong, I. Grundke-Iqbal, Tau in Alzheimer disease and related tauopathies, Curr. Alzheimer Res. 7 (2010) 656–664.

[2] G.G. Kovacs, Neuropathology of tauopathies: principles and practice, Neuropathol. Appl. Neurobiol. 41 (2015) 3–23.

[3] T. Arendt, J.T. Stieler, M. Holzer, Tau and tauopathies, Brain Res. Bull. 126 (2016) 238–292.

[4] M. von Bergen, P. Friedhoff, J. Biernat, J. Heberle, E.M. Mandelkow, E. Mandelkow, Assembly of tau protein into Alzheimer paired helical filaments depends on a local sequence motif (306VQIVYK311) forming β structure, Proc. Natl. Acad. Sci. U. S. A. 97 (2000) 5129–5134.
[5] F.A. Rojas Quijano, D. Morrow, B.M. Wise, F.L. Brancia, W.J. Goux, Prediction of nucleating sequences from amyloidogenic propensities of tau-related peptides, Biochemistry 45 (2006) 4638–4652.
[6] W.J. Goux, L. Kopplin, A.D. Nguyen, K. Leak, M. Rutkofsky, V.D. Shanmuganandam, D. Sharma, H. Inouye, D.A. Kirschner, The formation of straight and twisted filaments from short tau peptides, J. Biol. Chem. 279 (2004) 26868–26875.
[7] J. Zheng, C. Liu, M.R. Sawaya, B. Vadla, S. Khan, R.J. Woods, D. Eisenberg, W.J. Goux, J.S. Nowick, Macrocyclic beta-sheet peptides that inhibit the aggregation of a tau-protein-derived hexapeptide, J. Am. Chem. Soc. 133 (2011) 3144–3157.
[8] J. Zheng, A.M. Baghkhanian, J.S. Nowick, A hydrophobic surface is essential to inhibit the aggregation of a tau-protein-derived hexapeptide, J. Am. Chem. Soc. 135 (2013) 6846–6852.
[9] T. Mohamed, T. Hoang, M. Jelokhani-Niaraki, P.P. Rao, Tau-derived-hexapeptide 306VQIVYK311 aggregation inhibitors: nitrocatechol moiety as a pharmacophore in drug design, ACS Chem. Neurosci. 4 (2013) 1559–1570.
[10] M. Landau, M.R. Sawaya, K.F. Faull, A. Laganowsky, L. Jiang, S.A. Sievers, J. Liu, J.R. Barrio, D. Eisenberg, Towards a pharmacophore for amyloid, PLoS Biol. 9 (2011) e1001080.
[11] L. Lunven, H. Bonnet, S. Yahiaoui, W. Yi, L. Da Costa, M. Peuchmaur, A. Boumendjel, S. Chierici, Disruption of fibers from the Tau model AcPHF6 by naturally occurring aurones and synthetic analogues, ACS Chem. Neurosci. 7 (2016) 995–1003.
[12] S.A. Patil, R. Patil, S.a. Patil, Recent developments in biological activities of indanones, Eur. J. Med. Chem. 138 (2017) 182–198.
[13] J.C.J.M.D.S. Menezes, Arylidene indanone scaffold: medicinal chemistry and structure-activity relationship view, RSC Adv. 7 (2017) 9357–9372.
[14] M. Turek, D. Szczesna, M. Koprowski, P. Balczewski, Synthesis of 1-indanones with a broad range of biological activity, Beilstein J. Org. Chem. 13 (2017) 451–494.
[15] S. Radhakrishnan, R. Shimmon, C. Conn, A. Baker, Inhibitory kinetics of novel 2,3-dihydro-1*H*-inden-1-one chalcone-like derivatives on mushroom tyrosinase, Bioorg. Med. Chem. Lett. 25 (2015) 5495–5499.
[16] T.M. Kadayat, S. Banskota, P. Gurung, G. Bist, T.B.T. Magar, A. Shrestha, J.-A. Kim, E.-S. Lee, Discovery and structure-activity relationship studies of 2-benzylidene-2,3-dihydro-1*H*-inden-1-one and benzofuran-3(2*H*)-one derivatives as a novel class of potential therapeutics for inflammatory bowel disease, Eur. J. Med. Chem. 137 (2017) 575–597.
[17] R. Sheng, Y. Xu, C. Hu, J. Zhang, X. Lin, J. Li, B. Yang, Q. He, Y. Hu, Design, synthesis and AChE inhibitory activity of indanone and aurone derivatives, Eur. J. Med. Chem. 44 (2009) 7–17.

[18] F.-C. Meng, F. Mao, W.-J. Shan, F. Qin, L. Huang, X.-S. Li, Design, synthesis, and evaluation of indanone derivatives as acetylcholinesterase inhibitors and metal-chelating agents, Bioorg. Med. Chem. Lett. 22 (2012) 4462–4466.
[19] D.-D. Nan, C.-S. Gan, C.-W. Wang, J.-P. Qiao, X.-M. Wang, J.-N. Zhou, 6-Methoxy-indanone derivatives as potential probes for β-amyloid plaques in Alzheimer's disease, Eur. J. Med. Chem. 124 (2016) 117–128.
[20] L. Huang, H. Miao, Y. Sun, F. Meng, X. Li, Discovery of indanone derivatives as multi-target-directed ligands against Alzheimer's disease, Eur. J. Med. Chem. 87 (2014) 429–439.
[21] G.A. Parada, S.D. Glover, A. Orthaber, L. Hammarström, S. Ott, Hydrogen bonded phenol-quinolines with highly controlled proton-transfer coordinate, Eur. J. Org. Chem. (2016) 3365–3372.
[22] L. Li, M. Chen, F.-C. Jiang, Design, synthesis, and evaluation of 2-piperidone derivatives for the inhibition of β-amyloid aggregation and inflammation mediated neurotoxicity, Bioorg. Med. Chem. 24 (2016) 1853–1865.
[23] H.M. Sim, K.Y. Loh, W.K. Yeo, C.Y.Lee, M.L. Go, Aurones as modulators of ABCG2 and ABCB1: synthesis and structure-activity relationships, Chem. Med. Chem. 6 (2011) 713–724.
[24] H. Levine, Thioflavine T interaction with synthetic Alzheimer's disease β-amyloid peptides: detection of amyloid aggregation in solution, Protein Sci. 2 (1993) 404-410.
[25] L.P. Jameson, N.W. Smith, S.V. Dzyuba, Dye-binding assays for evaluation of the effects of small molecule inhibitors on amyloid (Aβ) self-assembly, ACS Chem. Neurosci. 3 (2012) 807-819.
[26] S.A. Hudson, H. Ecroyd, T.W. Kee, J.A. Carver, The thioflavin T fluorescence assay for amyloid fibril detection can be biased by the presence of exogenous compounds, FEBS J. 276 (2009) 5960-5972.
[27] G. Narang, D. P. Jindal, B. Jit, R. Bansal, B. S. Potter, R. A. Palmer, Formation of dimers of some 2-substituted indan-1-one derivatives during base-mediated cross aldol condensation, Helv. Chim. Acta 2006, 86(2), 258–264.
[28] C. Berthelette, C. McCooye, Y. Leblanc, L. A. Trimble, N. N. Tsou, Studies on the dimerization of 2-benzylidene-1-indanone, J. Org. Chem. 62 (1997) 4339–4342.
[29] T. M. Kadayat, S. Banskota, P. Gurung, G. Bist, T. B. T. Magar, A. Shrestha, J.-A. Kim, E.-S. Lee, Discovery and structure-activity relationship studies of 2-benzylidene-2,3-dihydro-1H-inden-1-one and benzofuran-3(2H)-one derivatives as a novel class of potential therapeutics for inflammatory bowel disease, Eur. J. Med. Chem. 137 (2017) 575–597.
[30] Z. Wei, Y. Wang, Y. Li, R. Ferraccioli, Q. Liu, Bidentate NHC-cobalt catalysts for the hydrogenation of hindered alkenes, Organometallics 39 (2020) 3082–3087.
[31] H. M. Sim, K. Y. Loh, W. K. Yeo, C. Y. Lee, M. L. Go, Aurones as modulators of ABCG2 and AABCB1: synthesis and structure –activity relationships, Chem. Med. Chem. 6 (2011) 713–724.
[32] M. P. Carrasco, A. S. Newton, L. Gonçalves, A. Góis, M. Machado, J. Gut, F. Nogueira, T. Hänscheid, R. C. Guedes, D. J.V.A. dos Santos, P. J. Rosenthal, R. Moreira, Probing the aurone

scaffold against Plasmodium falciparum: design, synthesis and antimalarial activity, Eur. J. Med. Chem. 80 (2014) 523–534.
[33] O. Fedorova, G. E. Jagdmann Jr., R. L. Adams, L. Yuan, M. C. Van Zandt, A. M. Pyle, Small molecules that target group II introns are potent antifungal agents, Nat. Chem. Biol. 14 (2018) 1073–1078.
[34] R. Haudecoeur, A. Ahmed-Belkacem, W. Yi, A. Fortuné, R. Brillet, C. Belle, E. Nicolle, C. Pallier, J.-M. Pawlotsky, A. Boumendjel, Discovery of naturally occurring aurones that are potent allosteric inhibitors of hepatitis C virus RNA-dependent RNA polymerase, J. Med. Chem. 54 (2011) 5395–5402.
[35] M. Zhang, G.-Y. Chen, T. Li, B. Liu, J.-Y. Deng, L. Zhang, L.-Q. Yang, X.-H. Xu, Synthesis and herbicidal evaluation of 4,6-dimethoxyaurone derivatives, J. Heterocycl. Chem. 52 (2015) 1887–1892.
[36] R. Haudecoeur, A. Gouron, C. Dubois, H. Jamet, M. Lightbody, R. Hardré, A. Milet, E. Bergantino, L. Bubacco, C. Belle, M. Réglier, A. Boumendjel, Investigation of binding-site homology between mushroom and bacterial tyrosinases by using aurones as effectors, Chem. Bio. Chem. 15 (2014) 1325–1333.
[37] Schrödinger Release 2019-2: Maestro, LigPrep, Schrödinger, LLC, New York, NY, 2019.
[38] http://OpenMOPAC.net
[39] J.J.P. Stewart, Optimization of parameters for semiempirical methods VI: more modifications to the NDDO approximations and re-optimization of parameters, J. Mol. Modeling 19 (2013) 1–32.
[40] Jmol: an open-source Java viewer for chemical structures in 3D. http://www.jmol.org